Sol-gel ZnO Nanoparticles as a Selective Electron Layer in low- Temperature Solution-Processed Perovskite Solar Cells.

Ahmed. H. Kurda [1]
Department of Physics, College of Science Salahaddin University
Erbil, Kurdistan of Iraq.
Email: ahmedkurda.69@gmail.com

Yuosif M. Hassan [2]
Department of Physics, College of Science
Salahaddin University
Erbil, Kurdistan of

Naser M. Ahmed [3]
School of Physics, University Sains Malaysia, Nano optoelectronics Research &Technology (NORT)
11800,Penang, Malaysia

***Abstract*:**The sol-gel ZnO nanoparticles were found to form a relatively compact film without sintering steps throw low temperature process (<120^{0}C) to perform perovskite solar cells using a spin coating technique. The perovskite layer was sandwiched between zinc oxide (ZnO) nanoparticles thin film as a selective electron transport layer (ETL) and organic hole selective poly (3,4-ethylenedioxythiophene): poly (styrenesulfonate) PEDOT:PSS layer. A methylam-moniom lead iodide (CH_3NH_3) PbI_3 active layer was deposited on the ZnO nanoparticles modified ITO substrate. X-Ray Diffraction (XRD), field effect scanning electron microscope (FESEM) were employed to characteristic structure and morphology of the samples. Photoluminescence (PL) spectroscopy used for optical band gap energy for ZnO nanoparticles, methyl ammonium lead iodide (CH_3NH_3)PbI_3 perovskite were calculated to be 3.27, 1.62 eV respectively. The crystalline ZnO nanoparticles 15 nm in diameter were determined by transmission electron microscope (TEM). The whole device could be fabricated under mild conditions with relatively low temperature and solution process. Devices based on modified (ETL) could achieve high power conversion efficiency (PCE) 7.41 on rigid and 4.65 on flexible substrates with improved device stability. These results imply that interface engineering provides a promising approach to simplify device configuration and reduce the fabrication cost for perovskite solar cells

***Keywords**: ZnO, nanoparticles, low- temperature, Spin Coating, perovskite, solar cells.*

I. INTRODUCTION

Low- temperature solution process able hybrid solar cells are becoming more attractive as they offer a viable alternative to conventional solar cells fabricated via vacuum-based or high-temperature processes for large-scale, and cost-effective manufacturing on flexible plastic substrates. Organic-inorganic an interesting class of materials is extremely studied as the hybrid, which are required to combine the attractive feature of organic materials and inorganic materials within a single molecule-scale composite.

In the past two decades the organic inorganic hybrid perovskite have arisen as a new functional material and have grown great attention and research effort when deposited by spin coating. These compounds are self-assembled system; they form a multi-quantum well structure spontaneously and exhibit excellent optical and electronic properties at room temperature. The optical properties of these materials can be finely tuned thanks to molecular engineer on the organic part or on the inorganic part. Furthermore, the preparation of these materials is a very simple compared to the deposition techniques for inorganic semiconductors such as PECVD (Plasma Enhanced Chemical Vapour Deposition), MBE (Molecular Beam Epitaxy), and MOCVD (Metalorganic Chemical Vapour Deposition).

Recently organic in organic perovskite have been used in many optoelectronic devices such as surface Plasmon's [1, 2], LEDs [3], solar cells [4-6], and Microcavities [7-9]. The

interesting optical and electrical properties of perovskite along with the low cost processing make them strong potential candidates to be applied to optoelectronic devices. The basic structure of the organic inorganic perovskites is AMX_3, A- is typically an anion (X = Halogens, I, Cl, Br), (M is generally divalent metal; Pb, Sn, Co. Methylammonium lead iodide $(CH_3NH_3)PbI_3$ has proven to be one of most promising in low cost photovoltaic. A phenomenal increases in device performance has been achieved within a span of few year [10-15] because of their excellent optoelectronics properties such as; carrier life time, high mobility, low band gap (1.5 - 2.3 eV), long diffusion time via a facial cheap process synthesis [16-19].

Here we report synthesis sol-gel Zn0 nanoparticles as an electron transport layer in perovskite solar cells, the hydrothermal method used for preparation ZnO nanoparticles, tow-step method solution processed synthesizes of (CH_3NH_3) PbI_3 perovskite thin films in low temperature ($< 120^{\circ}C$) by using the simplest technique spin coating deposition method. Photoluminescence (PL) method used to investigate the optical properties and measuring the energy gap for ZnO nanoparticles, perovskite thin films. For measuring the dimension of ZnO nanoparticles used transmission electron microscopy TEM. X-ray diffraction used for structure characterization. Field emission scanning electron microscope FESEM used for investigating the morphology in the perovskite solar cells and the current verses voltage (I-V) characteristics of device with different substrates were taken under Am1.5G (100 mW cm^{-2}) illumination.

II. EXPERIMENTAL SECTION

ZnO nanoparticles were prepared according to literature procedures [20]. Zinc acetate dehydrate (Zn $(COOH)_2.2H_2O$, Sigma Aldrich) 2.95 g was dissolved in methanol (125 ml) with stirring at 65 ^{0}C. A solution of potassium hydroxide (KOH) 1.48 g in methanol (65 ml) was then added drop wise at 60-65 ^{0}C over a period of 15 min. The reaction mixture was stirred for 2.5 h at 65 ^{0}C. After cooling to room temperature, the supernatant was decanted and the precipice was washed twice with methanol. Finally, ZnO nanoparticles were dispersed in the chloroform to form a ZnO nanoparticle solution. The solution was stable for more than a month.

Methylammonium iodide $(CH_3NH_3)I$ was synthesized by reacting 27.86 ml methylamine (40% in methanol, Sigma-Aldrich) and 30 ml of hydroiodic acid HI (57% in water, Sigma- Aldrich) in 250 ml round bottomed flask at 0 ºC for 2 h with stirring. The precipitate was recovered by evaporation at 50 ºC for 1h. The product, methylammonium iodide $(CH_3NH_3)I$ was washed with diethyl ether by stirring the solution for 30 min, which was repeated three times , and finally dried at 60 ºC in a vacuum oven for 24 h[21].

Solar cell fabrication: figure 1 shows the device architecture of the perovskite Solar cells were fabricated on rigid (glass/ITO, glass/ FTO) and flexible polyethylene terephthalate (PTE/ITO) substrates with a sheet resistances of 8 Ω sq^{-1} and 30 Ω sq^{-1} respectively. first, a ZnO nanoparticle layer was spin coated onto the substrate at 3000rpm for 20 s. the procedure was repeated three times to obtain a continuous smooth film. (CH_3NH_3) PbI3 was deposited on top of ZnO layer using a two-step method [21]. A 1 M lead iodide PbI_2 (Sigma, Aldrich) solution was prepared by dissolving 2.33g of PbI_2 in 5 ml of N, N-Dimethylformamid (DMF, Sigma Aldrich). The solution was kept at 70 ^{0}C for 2 h. A $(CH_3NH_3)I$ solution was prepared by dissolving 0.05 g of $(CH_3NH_3)I$ in 5 ml of 2-propanol (0.063M). A100µL portion of pbI_2 solution was dropped on the cleaned ITO (FTO) glass 2.5 × 2.5 cm^2 substrate; the substrata was spun immediately at 3000rpm for 20s and dried at 100 ^{0}C for 10 min. After cooled a 200µL of $(CH_3NH_3)I$ solution was dropped on the substrata; a wait time of 20 s was observed, and the sample was spun at 2000rpm for 20 s and dried at 100 ^{0}C for 10 min. The hole transporting layer was formed by spin –coating the PEDOT: PSS (37% in H_2O, Sigma Aldrich) at 3000rpm for 30 s and annealed at 120 ^{0}C for 10 min. Finally, a thick silver Ag layer was deposited by thermal evaporation at a base pressure of 4×10^{-5} mbar.

The optical properties of the samples were investigated using photoluminescence (PL) spectroscopy (model: jobinYvon 800 UV) with a wave length rang 200 -1100 nm and the optical band gap was measured from the peak of photoluminescence spectrum.

X-Ray diffraction XRD was used for the study of the crystalline structure of the perovskite thin films. XRD patterns were obtained with a (Model: PANalyticalX'pert PRO MRD PW 3040) single scan diffractometer with Cu Kα (λ= 1. 54056 Å) and scanning range of 2θ set between 20º and 80º. During the measuring, the current and the voltage of XRD were maintained at 40 mA and 36 KV respectively, and scan speed was 4º /min. Transmission Electron Microscopy (TEM) used for masuring the ZnO nanoparticle sizes. The field emission scanning electron microscope (FESEM) (Model: FEI Nova NanoSEM 450) was used for surface morphology characterization and the photovoltaic device (I-V) characterization was investigated by Forter Transient Measurement System.

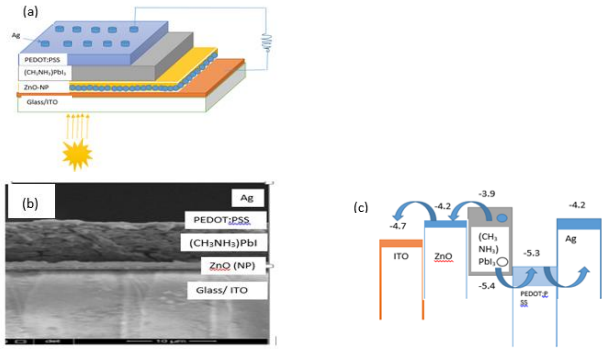

Fig. 1 Device architecture of glass/ITO/ZnO (NP)/Perovskite/PEODT: PSS/Ag. Solar cell (a) schematic of the device structure. (b) FESEM cros-section image of the device. (c) Energy level diagram.

III. RESULTSAND DISCUSSIONS:

A. Optical Properties of device

Figure 2a Shows the photoluminescence spectrum for ZnO nanoparticles. The samples are excited by a light source which is the 325 nm line of a He-Cd laser and the PL emission signal is then collected by a (spectrometer coupled to a CCD camera).The maximum intensity of the luminescence is observed at 378.315 nm corresponds the optical band gap E_g = 3.27 eV of ZnO nanoparticles. The small intensity peak is due to the same defects, in fact the values of band gap depend on many factors, e.g. the granular structure, the nature and concentration of precursors, the structural defects and the crystal structure of the films. Figure 1b shows the photoluminescence (PL) spectrum of the $(CH_3NH_3)PbI_3$ perovskite film, the sharp and smooth peak range from 700 nm to 800 nm with intensity over than 2000 c/sec appeared. The PL intensity is proportional to the number of the emitting photons on the perovskite surface. The maximum intensity of the luminescence is observed at wavelength 765.032 nm corresponds the optical band gap 1.62 eV for $(CH_3NH_3)PbI_3$ perovskite.

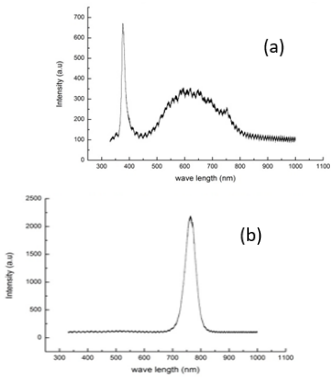

Fig. 2 The photoluminescence (PL) spectrum of (a) ZnO nanoparticles. (b) $(CH_3NH_3)PbI_3$ perovskite film on glass substrate.

B. Structural Analysis for device

Figure 3a depict the x-ray diffraction (XRD) pattern of the crystal structure and orientation of the ZnO nanoparticles on glass substrate using spin-coating 3000rpm and annelid at 120^0C for 10 min. From the XRD pattern, one can clearly observe a diffraction peak at 2θ =34.34.strong preferential growth is observed along c-axis i.e. (002), suggesting that the prepared ZnO nanoparticles have the wurtizit structure. Figure 3b depicts the X-ray diffraction (XRD) pattern perovskite film deposited on glass substrate using two-step solution deposition by spin-coating at 3000rpm and 2000rpm , and then annealed in air at 100ºC (Fig. 3(c)) . The XRD pattern of $(CH_3NH_3)PbI_3$ perovskite shows a set of strong diffraction peaks at 2θ=, 26.2611, 40.4942, and 50.4667 degree corresponding to the (110), (211), and (213) planes of the $(CH_3NH_3)PbI_3$ perovskite crystal, These indicate a tetragonal crystal structure of halide perovskite with high crystallinity using facile and attractive two-step deposition[22]. According to the literature [23], there is often a tiny signature peak at 2θ =34.2680 is corresponding to a low level impurity of PbI_2, and 2θ= 43.9415, 44.2250 are corresponding to $(CH_3NH_3)I$. The absence of a PbI_2 peak in the present perovskite film suggests complete consumption of PbI_2. XRD patterns could be ascribed comparable to the most reliable methods of vacuum deposition or vapour deposition processing [23].

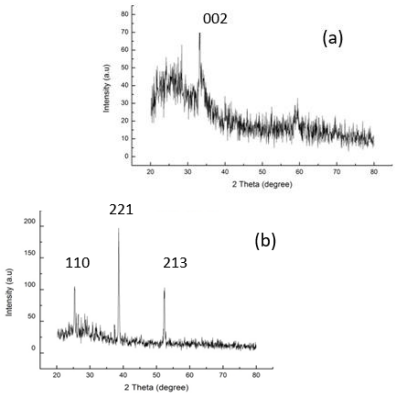

Fig. 3 the XRD of the (a) ZnO nanoparticle (b) $(CH_3NH_3)PbI_3$ perovskite thin film on glass substrate.

C. Morphological analysis of device

Figure 4 shows the transmission electron microscopy (TEM) of ZnO nanoparticles synthesized as electron selective contacts by hydrolysis method. The process produces a relatively compact ZnO layer and crystalline ZnO nanoparticles that are average 15 nm in diameter. The thickness of wich can be varied systematically by repeating the spin coating process several times.

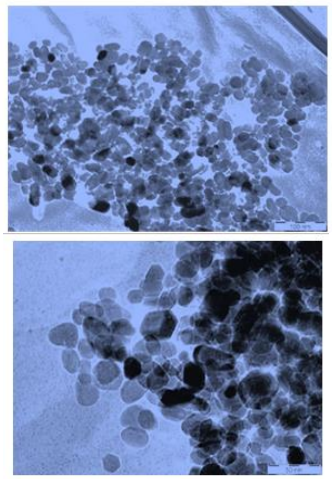

Fig.4 Transmission Electron Microscopy (TEM) of ZnO nanoparticles.

Figure 5a shows the top-view FESEM image of the ZnO nanoparticles deposited on glass substrate. Figure 5b shows the FESEM of PbI2 after spin coating on the zno nanoparticles, on the other hand, figure 5c shows the $(CH_3NH_3)PbI_3$ peroskite films fabricated using the two-step deposition method, we can clearly observe high uniformity and 100% coverage with smooth grain sizes of the perovskite films, this morphology highly similar to that of vapor-assisted solution-process [24].

In this work, a high concentration of PbI_2 solution in DMF is first spin coated on the substrate, which leads to more compact and uniform film, followed by spin coated the methylammonium iodide CH_3NH_3I solution in 2-propanol. During the second step, PbI_2 reacts with CH_3NH_3I to form $(CH_3NH_3)PbI_3$ perovskite. The two-step process takes advantage of PbI_2 being a layered-structure semiconductor and prone to intercalation reaction with methylamine.

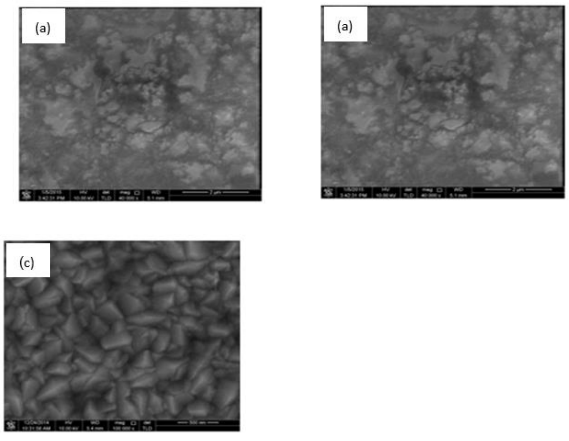

Fig. 5 the (FESEM) surface morphology for the (a) ITO/ZnO (NP). ((b) ITO/ZnO (NP)/PbI_2. (c) ITO/ZnO (NP) / $(CH_3NH_3)PbI_3$ perovskite.

IV. I-V CHARACTERIZATION OF DEVICE

Figure 6a presents the current - voltage (I-V) curves of the perovskite solar cells consisting of ZnO(nanoparticle)/$(CH_3NH_3)PbI_3$/PDOT:PSS/Ag on different (rigid glass /ITO, FTO and flexible PET/ITO substrates) under 1 sun Am 1.5 simulated solar irradiation. The photovoltaic parameters of the devices are summarized in **table 1**. As shown in figure 6b, the incident photon to electron conversion spectrum indicates that the device shows a spectral response in the region from the visible to near infrared (300 – 800 nm).

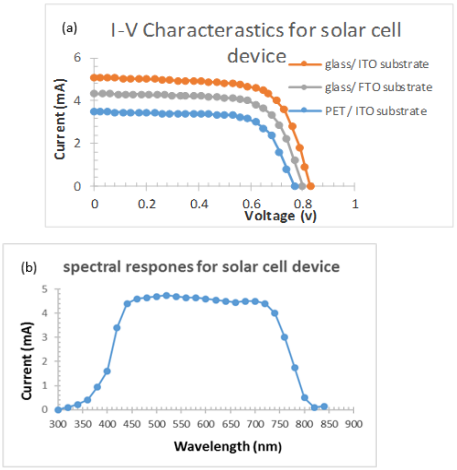

Fig. 6 (a) the current - voltage (I-V) curves of the perovskite solar cells. (b) The spectral response of solar cell device.

Table 1 Device parameters for solar cells prepared with varying substrates

substrates	I_{SC} (mA)	V_{oc} (Volt)	Fill factor %	PCE %
Glass/ ITO	12.8	0.83	70.0	7.41
Glass/FTO	10.85	0.8	68.5	5.94
PET/ITO	8.7	0.77	69.5	4.65

V. CONCLUSION

In this work ,we have synthesized ZnO nanoparticles as a selective electron layer in $(CH_3NH_3)PbI_3$ perovskite solar cells on rigid and flexible substrates using two-step solution processed spin-coating technique. The structure, morphological and optical properties of the films were investigated. The two -step solution is a simple technique, and there are many factors which affected the quality of the films. We have optimized deferent parameters such as time formation and full spin-coating deposition to obtain a good crystalline structure of $(CH_3NH_3)PbI_3$ perovskite film with intense and sharp (PL) peak. According to XRD results, the as-deposited films exhibited a tetragonal structure with (003) preferential orientation after annealing at 100 in air

ambiance for 10 min. The XRD pattern consists of two (003), (112) peaks which occurred due to $(CH_3NH_3)PbI_3$ crystals and grows along the c-axes. The grain size and thickness of the films are estimated to be 5.83 nm and 350 nm. FESEM of $(CH_3NH_3)PbI_3$ perovskite film shows that the medium grains made a smooth and opaque surface. The maximum photoluminescence (PL) spectrum intensity is observed at wavelength 378.315 nm, 765.032 nm corresponds to the optical band gap 3.27 eV for ZnO nanoparticles and 1.62 eV for $(CH_3NH_3)PbI_3$ perovskite film. A novel low-temperature approach to fabricated perovskite films, based on the kinetically favourable reaction between the as- deposited film of PbI_2 and CH_3NH_3I.The perovskite film derived from this approach exhibits full surface coverage, uniform grain structure with grin size up to nanometres, and 100% precursor transformation completeness. Two-stepdeposition presents a simple, controllable, and versatile approach to the pursuit of high-quality perovskite film and the resulting high-performance efficiency (PEC) 7.41 on rigid and 4.65 on flexible perovskite solar cells.

ACKNOWLEDGMENT

The athuors thanks the finantional support for splite- site program salhaddin university,Higher Education Minestery fo Kurdistan rigen of Iraq and the University Sains Malaysia (USM) in Malaysia for completing this research.

REFERENCES

[1] C. Symond, J. Bellessa, J. C. Plenet, A. Brehier, R. S. Lauret, and E. Deleporte. Emission of Hybrid Organic-inorganic Exaction/Plasmon Mixed States. Appl. Phys. Lett 90(9), (2007), 6951-5656.

[2] C, Symond, J. Bellessa, J. C. Plenet, A. Brehier, R. S. Lauret, and E. Deleporte. Particularities of Surface Plasmon- Exaction Strong Coupling with Large Rabi Splitting. New J. Phys., 10, (2008), 2630-2636.

[3] M. Era, S. Morimoto, T. Tsutsui, and S. Saito. Organic-Inorganic Hetrostructure Electroluminescent Device Using a Layered Perovskite Semiconductor $(C_6H_5C_2H_4NH_3)_2PbI_4$. Appl. Phys. Lett., 65(6) August (1994), 676-688.

[4] A. Kojima, K. Teshima, Y. Shirai, and T. Miyasaka. Organometal Halide Perovskites as Visible – light Sensitizers for Photovoltaic cells. Journal of the American Chemical Society, 131 (17), (2009), 6050-6054.

[5] C.R. Li, H.T. Deng,J. Wan,F. Levy, and W. J. Photoconductive Properties of Organic –Inorganic Hybrid Perovskite Nanocomposities Devise Structure. Material Letters, 64(24), (2010), 2735-2737.

[6] I. Koutselas, P. Bampoulis, E. Maratou, T. Evagelinou, G. Pagona, and G .C. Papavas Siliou. Some Unconventional Organic-inorganic Hybrid low-dimensional Semiconductors and Related light- emitting Devices. The Journal of Physical Chemistry C, 115(17), (2011), 8475-8483.

[7] G. Lanty, J. S. Lauret, E. Deleporte, S. Bouchoule, X. Lafosse. Uv Polaitonic Emission from a Perovskite-based Microcavity. Appl. Phys. Lett., 93(8), (2008) 6951-6955.

[8] A. Brehier, R. Parashkov, J. S. Lauret, and E. Deleporte. Strong Exciton-photon coupling in a Microcavity Containing Layered Perovskite Semiconductors. Appl. Phys. Lett., 89, (2006), 1711-1715.

[9] Y. Wei, J. S. Lauret, L. Galmiche, P. Audebert and E, Deleport. Optics Express, 20, 10402, (2012).

[10] P.V. Kamat. Evolution of Perovskite and Decrease in Energy Payback Time. J. Phys. Chem. Lett., 4, (2013), 3733-3734.

[11] G. Hodes, D. Cahen. Photovoltaics Cells Roll Forward. Nat. Photonics 8, (2014), 87-88.

[12] G. Hodes. Perovskite-based Solar Cells. Science 342, (2013), 317-318.

[13] j. bisquert. The Swift Surge of Perovskite Photovoltaics. J. Phys. Chem. Let. 4, (2013), 2597-2598.

[14] G. N. park. Organometal Perovskite Light Absorbers toward a 20% efficiency Low- Cost Solid Stat Mesoscopic Solar Cell. J. Phys. Chem. Let. 4, (2013), 2423-2429.

[15] H. J. Snaith. Perovskite the Emergence of a New Era for Low-Cost, High-Efficiency Solar Cells. J. Phys. Chem. Lett. 4, (2013), 3623-3630.

[16] S. D. Stranks, G.E Eperon, G. Grancini, C. Menelaou, M. J. P. Alcocer, T. Leijtensl. M. Herz, A. Petrozza, H. J. Snaith. Electron-Diffusion Lengths Exceeding 1 Micrometre in an Organometal Trihalide Perovskite Absorber. Science 342, (2013), 3623-3630.

[17] H. S. kim, I. Mora-Sero, V. Gonzalez-Pedro, F. Fabegat-Santiago, E. J. Juarez-Perez, N. G. Park, J. Bisquert. Mechanism of Carrier Accumulation in Perovskite Thin – Absorber Solar Cells. Nat. Commune. 4, (2013), 2242-2246.

[18] G. Xing, N. Mathews, S. Sun, S. S. Lim, Y. M. Lam, M. Gratzel, S. Mhaisalkar, T.C. Sum. Long-Rang Balanced Electron-and Hole- Transport Length in Organic-Inorganic $(CH_3NH_3)PbI_3$. Science. 342, (2013), 342-347.

[19] Y. Zhao, A. M. Nardes, K. Zhu. Solid- State Mesostructured Perovskite $(CH_3NH_3)PbI_3$ Solar cells: Charge Transport, Recombination, and Diffusion Length. J. Phys. Chem. lett.5, (2014), 490-494.

[20] J. H. Im, C. R. Lee, J. W. Lee, S. W. Park and N. G. Park, 6.5% efficient perovskite quantum- dot-sensitized solar cell. *Nanoscale* **3** (2011) 4088 - 4093.

[21] J. Burschka, N. Pellet, S-J. Moon, M. Gratzel, sequential deposition as arout to high-performance perovskite-sensitized solar cells. *et al*. *Nature* **499** (2013) 316 -319.

[22] Sh. Yang *et al. Chem. Mater*. **26** (2014) 6705.

[23] M. Liu, M. B. Johnson and H. J. Snaith, Efficient planer hetrojunction perovskite solar cells by vapour deposition. *Nature* **501** (2013) 395-398.

[24] Q. Chen, H. Zhou, G. li and Y. Yang. Planer hetrojunction perovskite solar cells via vapour- assisted solution process. *J. Am. Chem. Soc*. **15** (2014) 136 -138.